



## Regular article

# Extracellular electron transfer-enhanced sulfamethoxazole biodegradation: Mechanisms and process strengthening



Oluwadamilola Oluwatoyin Hazzan <sup>a,b</sup>, Collins Chimezie Elendu <sup>c</sup>, Claude Kiki <sup>a,b</sup>, Geng Chen <sup>a,b</sup>, Juven Sugira Murekezi <sup>a,b</sup>, Asmamaw Abat Getu <sup>a,b</sup>, Yong Xiao <sup>a,b,\*</sup>

<sup>a</sup> CAS Key Laboratory of Urban Pollutant Conversion, Institute of Urban Environment, Chinese Academy of Sciences, Xiamen, Fujian 361021, PR China

<sup>b</sup> University of Chinese Academy of Sciences, Beijing 100049, PR China

<sup>c</sup> Xinjiang Institute of Ecology and Geography, Chinese Academy of Sciences, Urumqi, Xinjiang, PR China

## ARTICLE INFO

## ABSTRACT

## Keywords:

Antibiotic degradation  
Bioelectrochemical system  
*Shewanella oneidensis* MR-1  
Sulfamethoxazole

Antibiotics like Sulfamethoxazole (SMX) pose a significant threat to public health and environmental well-being. To address this issue, effective strategies are being developed to remove antibiotics from the environment. This study investigates the degradation of SMX with a focus on elucidating the mechanism by which extracellular electron transfer (EET) enhances the efficient degradation of the antibiotic. The results show that SMX was significantly degraded (97 %) by *Shewanella oneidensis* MR-1 after 120 hours in the presence of a bioelectrochemical system (BES) at a concentration of 1 mg L<sup>-1</sup>, compared to the absence of BES (69 %) at the same concentration and time. BES was observed to simultaneously remove pollutants like SMX while generating electricity at this concentration. Proteomic analysis was further employed to clarify the mechanism behind this process. Three key SMX-degrading proteins; S-ribosylhomocysteine lyase (luxS), Deoxyribose-phosphate aldolase (deoC), and Amidohydrolase which mainly participated in C-S cleavage, S-N hydrolysis and isoxazole ring cleavage were identified. The study demonstrates that *S. oneidensis* MR-1 can promote the generation of Nicotinamide Adenine Dinucleotide and Adenosine Triphosphate and facilitate electron transfer to enhance the efficient degradation of SMX. The findings of this study provide new insights into the correlation mechanism between SMX degradation and EET, ultimately contributing to innovative solutions for environmental remediation.

## 1. Introduction

Sulfamethoxazole (SMX) is a commonly employed antibiotic from the sulfonamide class, which exhibits broad-spectrum activity against both gram-negative and gram-positive microorganisms [1] and it is used to treat a range of human infections such as urinary tract infections, bronchitis and prostatitis. Furthermore, it is employed in veterinary medicine and aquaculture to manage bacterial infections in animals and aquatic organisms [2]. Prolonged use of SMX can lead to adverse effects, including thyroid dysfunction, increased cancer risk and kidney damage. Similarly, its prolonged exposure to natural water bodies can lead to the emergence of antibiotic-resistant bacteria, which present a critical risk to aquatic ecosystems and potentially harm human health [3–7]. Therefore, developing a cost-effective and efficient treatment solution for SMX is crucial to mitigate its negative impacts.

Different treatment processes ranging from physical, biological, and chemical methods exist for the treatment of pollutants like SMX. However, these methods possess some challenges such as high cost, time-consuming and might generate a more toxic product compared to the parent compound. Similarly, wastewater treatment plants (WWTPs) are not designed for antibiotic removal [8] as such, Bioelectrochemical systems (BESs) are being explored as a viable solution for breaking down difficult-to-degrade contaminants like SMX [9] and therefore have attracted significant attention in pollutant degradation [10], where the microbe participates in the detoxification of organic contaminants and can exchange electrons with the electrode, i.e. the process of extracellular electron transfer (EET) [11]. Many bacteria such as *Shewanella*, *Geobacter*, *Desulfuromonas*, *Aeromonas*, and *Paleobacter* have been identified as microorganisms capable of EET. Among them, *Shewanella oneidensis* MR-1 stands out as a prominent model organism due to its

\* Corresponding author at: CAS Key Laboratory of Urban Pollutant Conversion, Institute of Urban Environment, Chinese Academy of Sciences, Xiamen, Fujian 361021, PR China.

E-mail address: [yxiao@iue.ac.cn](mailto:yxiao@iue.ac.cn) (Y. Xiao).

ability to adapt to various respiratory modes, its diverse metabolic capabilities, and the ease with which its genetic makeup can be studied [12].

Several research studies have investigated the biodegradation of SMX by this model organism [13–19]. Most research has focused on understanding the overall biodegradation process. For example, the study by Mao et al. [13] assessed and characterized sulfonamide degradation by *S. oneidensis* MR-1 and evaluated the potential of the strain for application in the removal of sulfonamides from contaminated environments. Similarly, the research by Lin et al. [19] on EET in *Shewanella oneidensis* MR-1 focused on strategic genetic manipulation to improve the capabilities associated with EET in MR-1. Few studies have focused on the mechanism of how EET enhances the efficient degradation of SMX. As a result, this study leverages this while also using proteomics as a technique to clarify the mechanism. The study proposed four degradation pathways for SMX. SMX underwent initial degradation via a hydroxylation process, which resulted in N-S (Pathway I) and C-S (Pathway II) bond cleavage. Pathway III was generated as a result of the cleavage of the S-C bond catalyzed by S-ribosyl homocysteine lyase encoded by gene luxS and pathway IV occurred via nitro-substitution on the amino group of SMX. The key proteins involved in SMX degradation and the possible correlation mechanism between the evolution of EET function and the degradation of SMX were identified. This study provides insight into the complex relationships between SMX degradation and EET, ultimately opening up new avenues for pioneering environmental remediation strategies.

## 2. Materials and methods

### 2.1. Preparation of the bacteria culture and composition of the culture medium

This experiment used gram-negative bacteria *S. oneidensis* MR-1 as the research object. The model organism was provided by the Key Laboratory of Urban Pollutant Conversion, Institute of Urban Environment, Chinese Academy of Sciences. Cultures were prepared from 5 mL frozen stock suspensions in equal parts of glycerol (50 %) maintained at  $-80^{\circ}\text{C}$ . The thawed cell culture was transferred to Erlenmeyer flasks with Luria-Bertani (LB) medium in a sterile fume hood and then incubated aerobically at  $30^{\circ}\text{C}$  in a rotary shaker at 150 r/min for 12 h. LB consisted of tryptone (10 g/L), yeast extract (5 g/L), and NaCl (10 g/L), adjusted to 7.0 pH using NaOH. The cultures were then washed twice with sterile saline (NaCl, 0.9 %) by centrifugation (5000 g, 5 min). The supernatant was discarded, and the cells were suspended in the medium required for the subsequent experiment.

The bacteria after being grown from frozen stocks were transferred into the anaerobic medium containing (per-litre): 0.31 g NH<sub>4</sub>Cl, 10.32 g Na<sub>2</sub>HPO<sub>4</sub>, 3.32 g Na<sub>2</sub>PO<sub>4</sub>, 0.13 g KCl, 0.1 g CaCl<sub>2</sub>, 0.1 g MgSO<sub>4</sub>·7 H<sub>2</sub>O plus 10 mL of a mineral mix (containing per litre: 1.5 g NTA, 0.1 g MnCl<sub>2</sub>·4 H<sub>2</sub>O, 0.3 g FeSO<sub>4</sub>·7 H<sub>2</sub>O, 0.17 g CoCl<sub>2</sub>·6 H<sub>2</sub>O, 0.1 g ZnCl<sub>2</sub>, 0.04 g CuSO<sub>4</sub>·5 H<sub>2</sub>O, 0.005 g ALK(SO<sub>4</sub>)<sub>2</sub>·12 H<sub>2</sub>O, 0.005 g H<sub>3</sub>BO<sub>3</sub>, 0.09 g Na<sub>2</sub>MoO<sub>4</sub>, 0.12 g NiCl<sub>2</sub>, and 0.02 g NaWo<sub>4</sub>·2 H<sub>2</sub>O). The medium was adjusted to pH 7. Filter-sterilized casamino acids were added (0.002 %) after autoclaving plus 1 mL of vitamin (containing per liter: 0.005 g 4 Aminobenzoic acid (Folate), 0.001 g D (+) biotin (Vitamin H), 0.01 g Nicotinic acid (Vitamin B3), 0.0025Ca-D (+) pantothenate (Vitamin B5), 0.025 g Pyridoxamine dihydrochloride (Vitamin B6), 0.005 g Thiaminum dichloride (Vitamin B1), 0.005 g Cyanocobalamin (Vitamin B12). Lactate (20 mM) was added as the sole carbon source.

### 2.2. Chemicals and analytical methods

All chemicals and reagents including SMX, methanol (HPLC grade), formic acid, and acetonitrile (HPLC grade) used for this experiment were of analytical (purity  $\geq 98\%$ ) grade and were purchased from Aladdin Industrial Corporation, China. The stock solution of SMX was prepared

by dissolving the compound in ultrapure water, followed by a 72-hour stirring period in the absence of light. The basic properties of SMX are presented in Table S1.

### 2.3. BES configuration and operation

Wide-mouth glass bottles were used as the reactor with the lid having a three-hole rubber plug. All experiments were carried out in triplicates and under anaerobic conditions. The reactor adopted a three-electrode system. Both the counter electrode and the working electrode were carbon felt (obtained from Gansu Haoshi Carbon Fibre Co Ltd..., China) with a dimension of  $2 \times 2$  cm for the working electrode and  $2 \times 3$  cm for the counter electrode. The reference electrode was potassium chloride (KCl) (Saturated KCl from Shanghai Chenhua Company, China). Electrodes were rinsed with acetone, cleaned with 75 % ethanol, and stored in deionized water. The electrochemical station CHI1000C with 6 channels was operated at a constant potential of +0.2 V, a room temperature of about  $28^{\circ}\text{C}$ . The schematic diagram of the three-electrode BESs is presented in Fig. 1.

To determine the concentration at which *S. oneidensis* MR-1 could degrade SMX more efficiently, varying initial SMX dosages of 1, 2, 10 and 20 mg L<sup>-1</sup> were placed in the 100 mL medium in wide-mouth glass bottles. The operation cycle was carried out by inoculating *S. oneidensis* MR-1 (1 %, v/v) into the culture medium. The cycle ran for 5 days and the SMX removal rate was evaluated.

### 2.4. SMX degradation without BES

The evaluation of SMX degradation for this experiment was conducted in 100 mL serum bottles. The medium was ventilated with high-purity nitrogen gas (A three-step aeration technique) [20] and tightened with butyl stoppers to ensure the absence of oxygen. The serum bottles were inoculated with 1 % pure *S. oneidensis* MR-1 with similar initial SMX dosages as that of the BES. Incubation was performed in a rotary shaker set at a speed of 150 r/min at a temperature of  $30^{\circ}\text{C}$  for 120 hours.

### 2.5. Analytical methods

Daily sampling was conducted for 5 days, during which the supernatant was filtered using a membrane filter with a pore size of 0.22  $\mu\text{m}$  before analysis. The samples with 1 mg L<sup>-1</sup> initial SMX dosage, were analysed with liquid chromatography-mass spectrometry (LC-MS/MS) (Shimadzu, Japan). The chromatographic separation was achieved using mobile phases consisting of a mixture of 0.1 % formic acid in water (A) and methanol (B). A chromatographic column of Kinetex C18 (4.6  $\times$  100 mm, 2.6  $\mu\text{m}$ , Phenomenex, CA, USA) was used at a flow rate of

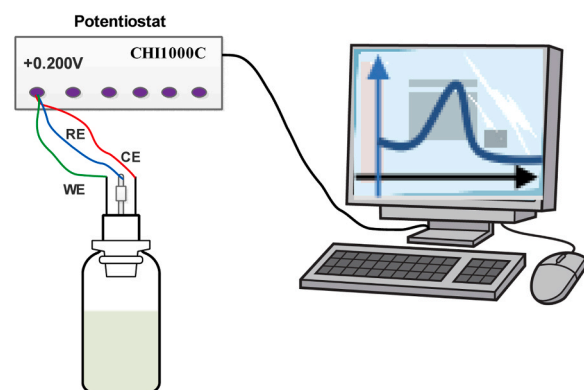


Fig. 1. Schematic diagram of three-electrode bioelectrochemical system (BES). WE, RE and CE represent the working electrode, reference electrode and counter electrode respectively.

0.80 mL min<sup>-1</sup>, column temperature of 40 °C and an injection volume of 10 µL. The samples corresponding to the initial SMX dosages of 2, 10 and 20 mg L<sup>-1</sup> were analysed using High-Performance Liquid Chromatography (HPLC) (Hitachi L-2000 series; Hitachi, Japan) which featured a UV/visible detector set at a wavelength of 269 nm and an Agilent Zorbax Eclipse plus C18 column with a dimension of 4.6 × 250 mm, 5 µm. The mobile phase composition consisted of 0.017 mol L<sup>-1</sup> phosphoric acid aqueous solution (A) and acetonitrile (B). The chromatographic analysis was conducted under the following conditions: a flow rate of 1.0 mL/min, a column temperature of 30 °C, with an injection volume of 10 µL.

## 2.6. Kinetics and statistical analysis

A pseudo-first-order kinetic model was employed to describe the rate of antibiotic removal over time [21] as shown in Eq. (1).

$$-\ln\left(\frac{A_r}{A_0}\right) = k \times t \quad (1)$$

$A_0$  and  $A_r$  are given as the initial and residual antibiotic concentrations at a given time  $t$ , respectively. The degradation rate constant ( $k$ ) was determined by Eq. (2)

$$k = -\ln\left(\frac{A_r}{A_0}\right)/t \quad (2)$$

Data analysis was performed using Excel 2010, GraphPad Prism 8.0, and Origin software. The results are expressed as the mean value ± standard deviation. The significance of the findings was evaluated using a statistical threshold of  $p < 0.05$ , indicating that any  $p$ -values less than this threshold were deemed statistically significant.

## 2.7. Label-free quantitative proteomic analysis

Proteins were isolated from bacterial samples under conditions with and without BES. The protein expression levels in the samples with and without BES were determined using label-free quantitative proteomics analysis. This approach is a mass spectrometry-based technique for protein identification and quantification in biological samples. It allows for the evaluation of variations in protein expression across different samples, facilitating detailed analysis of biological processes [22]. The analysis was conducted by Shanghai Applied Protein Technology Co. Ltd (Shanghai, China). The database used was the “uniprot” public database (<http://www.uniprot.org/>) and 76417 sequences. The identified proteins were annotated using the Gene Ontology (GO), Kyoto Encyclopedia of Genes and Genomes (KEGG), and Clusters of Orthologous Groups (COG) databases, which enabled the evaluation of their functional properties and roles. The primary aim of the GO is to systematically arrange functional information about genes, enabling the characterization of each gene based on its functions through GO annotations and terms. GO annotations for each gene are available in prominent databases such as the National Center for Biotechnology Information (NCBI) Gene database, Ensembl, and other major gene information repositories [23]. While the GO describes gene functions across three main domains: molecular functions (MF), biological processes (BP) and cellular components (CC) [24], the KEGG, which is also a knowledge base for systematic analysis of gene functions serves primarily as a bioinformatics resource that links genomic data to higher-order biological functions. Its focus is on analyzing biological systems, pathways, and molecular interactions, facilitating the understanding of cellular, organismal, and ecosystem functions through various interconnected databases [25]. The COG databases are specifically developed for the phylogenetic classification of proteins encoded in complete genomes. Each COG comprises proteins that are inferred to be orthologs, which are direct evolutionary counterparts typically found across different species. This classification facilitates a deeper understanding of protein function and

evolution among diverse lineages. The organisation of proteins into clusters based on their evolutionary relationships makes it possible to make inferences about gene functions and the evolutionary processes that influence genome diversity [26]. In this study, proteins with upregulated and downregulated expressions were screened when fold change was  $\geq 2$  and  $P$  value  $\leq 0.05$ . Protein-protein interactions were inferred using the STRING database, which provides a comprehensive platform for predicting protein-protein interactions (<http://string.embl.de/>).

## 2.8. Identification of SMX transformation products (TPs)

The intermediates produced by microbial metabolic pollutants during the reaction were identified by LC-MS/MS. The target substance was separated by the Kintex C18 column. The liquid chromatography separation was performed using a mobile phase composed of 0.1 % formic acid (A) and methanol (B), with a flow rate of 0.2 mL/min. Electrospray ionization (ESI) was employed in both positive and negative ion modes in the process of material ionization.

## 2.9. Ecotoxicity assessment of the TPs

Evaluating the toxic effects of organic pollutants is crucial in regulating and managing environmental contaminants. The acute (short-term) and chronic (long-term) toxicity thresholds for the SMX antibiotics were predicted through computational methods [27,28], using Ecological Structure-Activity Relationship (ECOSAR).

Structure-Activity Relationship (ECOSAR) simulation software. With this, the potential risks associated with SMX and its metabolites were assessed for aquatic organisms using three different nutrient levels, which included Fish, Daphnids, and Green algae, as test species.

## 3. Results and discussion

### 3.1. Degradation performance of varying SMX concentrations

The degradation efficiency of SMX for the varying initial SMX dosages of 1, 2, 10 and 20 mg L<sup>-1</sup> both with BES and without BES is illustrated in Fig. 2. SMX degradation efficiency was determined to be 97 % and 69 %, 48 % and 35 %, 29 % and 19 %, 14 % and 13 % with and without BES for the different initial SMX dosages of 1, 2, 10, and 20 mg L<sup>-1</sup> respectively. At 1 mg L<sup>-1</sup> initial SMX dosage, the removal rate of SMX in BES after 5 days was determined to be 97 % while that without BES was 69 %. An increase in the SMX dosage to 20 mg L<sup>-1</sup>, led to a reduced removal efficiency of 14 % and 13 % with and without BES respectively. The kinetics fitting analysis is presented in Table 1. The SMX dosage of 1 mg L<sup>-1</sup> resulted in the highest degradation efficiency and thus subsequent experiments were performed at this concentration.

The concentration of antibiotics affects its treatment performance in BES. Guo, et al. [29] developed a BES to investigate chloramphenicol removal from wastewater at dosages of 10, 20 and 50 mg L<sup>-1</sup>. The findings of their study demonstrated that under the lower dosage of 10 mg L<sup>-1</sup>, almost all the chloramphenicol was removed after 36 hours while it took about 72 hours to completely remove chloramphenicol dosages of 20 and 50 mg L<sup>-1</sup>. In another study on the removal of metronidazole in microbial fuel cells (MFCs), at different concentrations of 0, 10, 30, and 50 mg/L, at 10 mg/L almost 85.4 % of metronidazole was removed within 24 hours of operation. At a dosage of 50 mg/L, the removal rate of metronidazole was significantly lower, with only 44 % of the substance being removed after 24 hours [30]. This indicates that metronidazole removal was significantly impaired at higher concentrations, suggesting a strong inhibition of the removal process. In the study by Xie, et al. [31], the degradation mechanism of SMX at different initial dosages of 0, 0.5, 5, and 50 mg/L in MFC was investigated. The study revealed that the maximum SMX removal efficiency achieved in MFCs was an impressive 98.4 % at a concentration of 5 mg L<sup>-1</sup> but at a

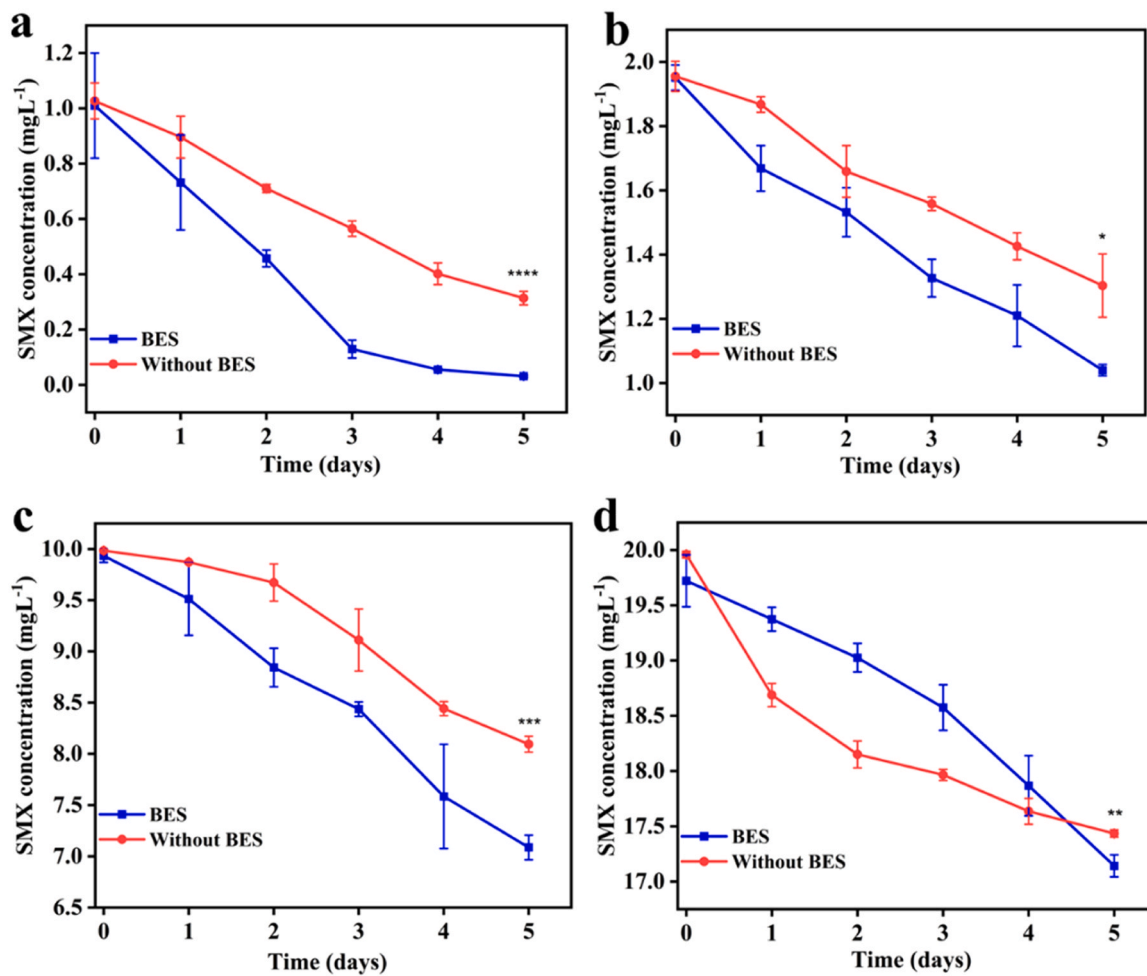


**Fig. 2.** Degradation efficiency of SMX with and without BES at (a)  $1 \text{ mg L}^{-1}$  (b)  $2 \text{ mg L}^{-1}$  (c)  $10 \text{ mg L}^{-1}$  (d)  $20 \text{ mg L}^{-1}$ . ns represents no statistically significant difference while the asterisks denote a statistically significant difference at  $p < 0.05$ .

**Table 1**  
Degradation kinetics parameters of SMX at different concentrations.

$C_0$ (mg/ L)	BES			Without BES		
	k	$t_{1/2}$	$R^2$	k	$t_{1/2}$	$R^2$
1	0.754 $\pm 0.045$	0.403 $\pm 0.026$	0.97	0.245 $\pm 0.012$	1.233 $\pm 0.062$	0.98
2	0.122 $\pm 0.008$	2.487 $\pm 0.156$	0.96	0.083 $\pm 0.008$	3.653 $\pm 0.339$	0.95
10	0.069 $\pm 0.002$	4.363 $\pm 0.108$	0.95	0.045 $\pm 0.001$	6.673 $\pm 0.176$	0.92
20	0.028 $\pm 0.002$	10.95 $\pm 0.863$	0.94	0.025 $\pm 0.001$	12.25 $\pm 0.238$	0.90

higher concentration of  $50 \text{ mg L}^{-1}$ , there was a decline in SMX removal to 84.4 %.

For this study, a comparative analysis of the two experimental conditions indicates that the reduction rates are generally higher in BES (Fig. 2) compared to the system without BES across all concentrations. In both conditions, the degradation efficiencies were seen to be lower at higher SMX concentrations and these results are consistent with previous reports as initially discussed, which indicates that the degradation efficiencies of antibiotics exhibit a certain degree of dependence on the initial concentration. This observation could potentially be attributed to the hormesis effect. The concept of hormesis describes a distinctive response to a substance, where the outcome is characterized by a dual effect. Specifically, low concentrations of the substance elicit salutary

consequences, while high concentrations trigger detrimental effects. The presence of a substantial quantity of a toxic substance such as SMX, can disrupt bacterial cells due to its ability to impede the production of folate, a crucial element in the synthesis of nucleic acids. Consequently, this inhibition hinders the growth and reproduction of the cells. Conversely, in instances when the concentration of the toxic substance is minimal, the inhibition of folate production may not occur, hence potentially facilitating microbial activity [32] and enhancing the degradation of the toxic substance at low doses compared to higher doses. It can therefore be inferred that when the initial concentration of SMX rises, the system's pollution load rises and more time is required to eliminate the antibiotics.

The kinetics fitting analysis was further used to explain the degradation of SMX. The results presented in Table 1 indicate that the reduction of SMX followed the first-order kinetics with  $R^2$  values all above 0.9 (0.92–0.99) thus indicating a strong correlation between the SMX reduction rate and its concentration. The first-order rate constants (k) in the BES decrease as the concentration of SMX increases. These results suggest that the reduction of SMX by *S. oneidensis* MR-1 in the BES is concentration-dependent. At  $1 \text{ mg L}^{-1}$ , the highest reduction rate is observed ( $k = 0.754 \pm 0.045$ ), suggesting that *S. oneidensis* MR-1 demonstrates the highest reduction efficiency for SMX at the lowest concentration tested in the BES. Similar to the system without BES, the first-order rate constants (k) in the system decrease with increasing SMX concentrations. The reduction of SMX by *S. oneidensis* MR-1 in the system without BES is also concentration-dependent, with lower rates at higher concentrations. Also, the highest reduction efficiency for SMX by

*S. oneidensis* MR-1 in the system without BES is observed at the lowest concentration tested. The half-lives of the antibiotics were shortest in BES ranging between 0.40 days to 10.95 days as presented in Table 1. For the system without BES, the half-life ranges between 1.23 days to 12.25 days. For both systems, SMX of initial concentration of 1 mg L<sup>-1</sup> has the shortest half-life and it continued to increase as the initial SMX concentration increased. These results indicate that a high concentration of antibiotics could inhibit its degradation process. Increased concentrations of antibiotics tend to inhibit microbial metabolic activities and thus lead to a reduction in the rate of antibiotic removal. The findings of this study have significant implications for understanding the microbial degradation of SMX under different conditions and may inform strategies for bioremediation applications.

### 3.2. Bioelectricity generation in BES

Based on the degradation results in Fig. 2, SMX exhibited the highest degradation efficiency in BES at the lowest concentration (1 mg/L) tested, necessitating an evaluation of the EET mechanism behind the enhanced degradation observed at this concentration. As such, the electricity generation capacity was examined at this concentration. The electricity generated from BES inoculated with *S. oneidensis* MR-1 is illustrated in Fig. 3. The control which is MR-1 without the antibiotic generated a peak electricity of about 7.6  $\mu\text{A cm}^{-2}$  (Fig. S1) which was consistent with previous reports [33], while the addition of SMX resulted in the production of a peak electricity density of 26.4  $\mu\text{A cm}^{-2}$  (Fig. 3).

Firstly, it was expected that SMX being an antibiotic would exert some degree of toxicity on the bacteria and thus would lead to a decline in the peak electricity production but this was not the case. This result suggests that *S. oneidensis* MR-1 was generating more electricity or engaging in increased electron transfer processes as a response to SMX. The increased electricity generation exhibited by MR-1 in response to SMX can be attributed to both metabolic adaptation and stress response mechanisms [34]. MR-1 utilizes EET pathways, such as the MtrCAB pathway, to carry out anaerobic respiration using various electron acceptors [35]. In this pathway, five key protein components have been identified: OmcA, MtrC, MtrA, MtrB, and CymA [36]. Current models regarding electron transfer in *S. oneidensis* MR-1 suggest that electrons generated from the oxidation of carbon sources are channelled through the menaquinone pool to the inner membrane-anchored c-type cytochrome CymA. From there, the electrons are transferred to the periplasmic c-type cytochrome MtrA, eventually reaching the outer membrane-bound c-type cytochromes MtrC and OmcA. These proteins interact with MtrB, an integral outer membrane scaffolding protein. The

outer membrane cytochromes then facilitate the reduction of various substrates. This EET capability possessed by the bacteria enables it to thrive in the presence of SMX thus demonstrating its versatility in adapting to environmental stresses.

### 3.3. Multifaceted analysis of the proteomics data

The Proteomics technique was used to clarify the mechanism of how EET enhances SMX degradation. The list of all the up and downregulated differentially expressed proteins is presented in Tables S2 and S3. The results in Fig. 2 show that BES has a significant effect on the degradation of SMX compared to the system without BES and as such the presence of BES might have introduced alterations in protein expression, and the proteomics analysis aimed to identify and characterize the differentially expressed proteins (DEPs) that result from these changes. For this analysis, the degradation of SMX in the BES was represented as BESSMX while SMX degradation without BES was represented as ASMX. The result of the proteomic analysis revealed 916 differentially expressed proteins (DEPs) with 552 upregulated proteins and 364 downregulated proteins (Fig. 4a). The volcano map of DEPs is presented in Fig. S2. The comparison between BESSMX and ASMX was visualized using a heatmap, which revealed distinct hierarchical clusters of proteins with analogous expression patterns (Fig. S3). The KEGG pathway analysis is presented in Fig. 4b. The KEGG pathway analysis indicates the various upregulated and downregulated functions associated with the antibiotic degradation process. Among the upregulated functions are histidine metabolism, biosynthesis of various antibiotics, styrene degradation and Hypoxia-inducible factor-1 (HIF-1) signalling pathway. The HIF-1 signalling pathway was demonstrated to be one of the upregulated pathways in the KEGG pathway analysis (Fig. 4b). HIF-1 is a crucial regulator of stress-induced gene expression, and while it is most responsive to hypoxia, its signalling can be influenced by various stimuli, including metabolic stress, growth factors, and molecules present in the extracellular matrix (ECM) [37]. Similarly, the upregulation of proteins involved in histidine metabolism processes such as hisI, and hisG explained a broader cellular response to stress induced by the presence of SMX. Proteins involved in histidine metabolism pathways (Fig. 4b) were discovered to be functionally linked to proteins involved in nitrogen metabolism. This could be because histidine is one of the amino acids involved in nitrogen cycling [38]. The upregulation of the histidine metabolism pathway may indicate a shift in nitrogen metabolism to accommodate the degradation of SMX or to utilize nitrogen-containing compounds generated during the degradation process. Another upregulated pathway in the KEGG pathway analysis is the pathway responsible for the biosynthesis of various antibiotics. The upregulation of this pathway can also be a cellular response to the environmental stress caused by the presence of SMX. Furthermore, the KEGG pathway analysis shows the downregulation of pathways such as that involved in other glycan degradation and nitrotoluene degradation. The downregulation of these pathways may indicate that the bacteria is diverting its metabolic resources and energy towards the pathways responsible for SMX removal and EET, thus leading to a decreased expression of pathways involved in the degradation of other compounds.

The KEGG pathway analysis of the top 20 proteins with the greatest fold enrichment is presented in Fig. S4 and the enriched pathway indicates that the pentose phosphate pathway (PPP) demonstrated the highest significance. The PPP is a crucial metabolic pathway that generates nicotinamide adenine dinucleotide phosphate (NADPH) and NADPH is an essential cofactor involved in various biosynthetic processes and redox reactions [39]. The significance of this pathway suggests that *S. oneidensis* MR-1 requires a substantial amount of NADPH to facilitate the degradation of SMX. NADPH is vital for cellular defence mechanisms, antioxidant responses, and reductive biosynthesis. The highest significance demonstrated by this pathway also indicates that *S. oneidensis* MR-1 utilizes the reducing ability generated through the PPP to support the breakdown of SMX and potentially cope with

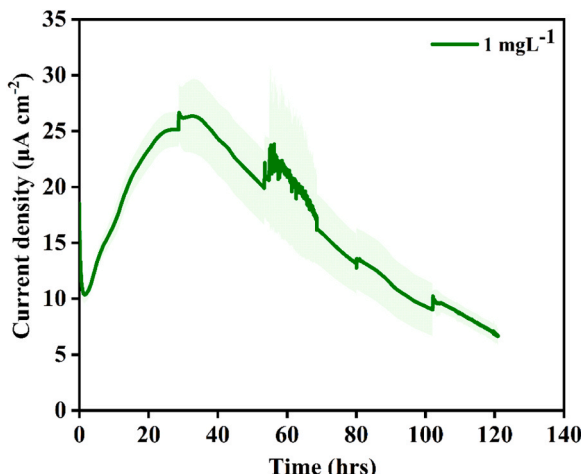
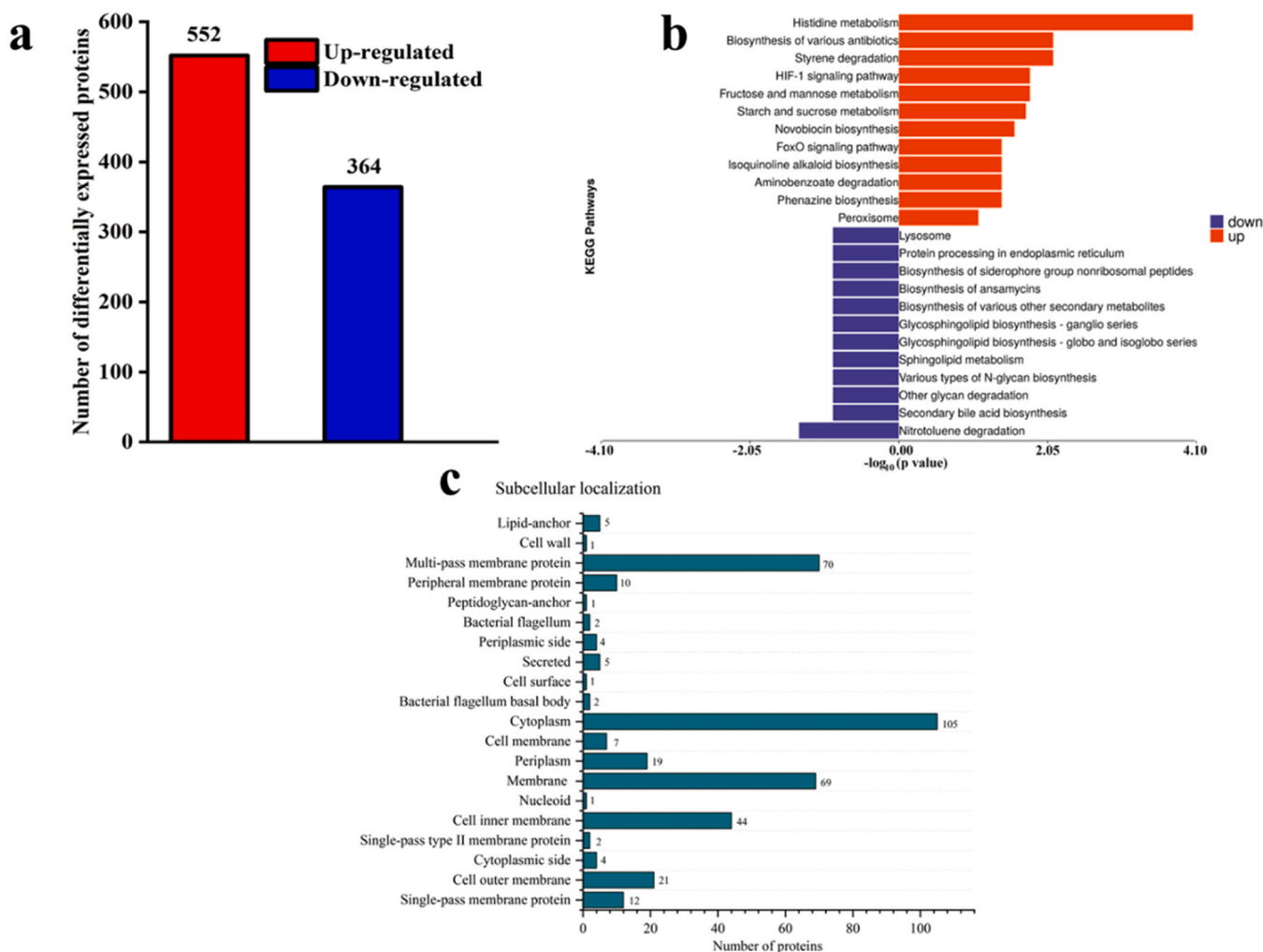


Fig. 3. Current generated from the working electrode of BES inoculated with *Shewanella oneidensis* MR-1 at SMX dosage of 1 mg L<sup>-1</sup>.



**Fig. 4.** (a) Numbers of differentially expressed proteins in *S. oneidensis* MR-1 in BESSMX vs. ASMX. The Red colour depicts overexpressed proteins while the blue colour depicts underexpressed proteins; (b) KEGG pathways showing the over and under-expressed functions. The orange colour depicts the overexpressed functions while the blue colour depicts the underexpressed functions; (c) Subcellular localization analysis.

oxidative stress induced by this process. Therefore, the highest significance demonstrated by the PPP in the degradation of SMX by *S. oneidensis* MR-1 signifies a coordinated metabolic response aimed at enhancing NADPH production and adapting to stress posed by the presence of the antibiotic.

The subcellular localisation result is presented in Fig. 4c and this result demonstrates that the majority of the DEPs are localised in key subcellular compartments, with 105 identified in the cytoplasm, 70 in multipass membrane proteins, 69 in the membrane, and 44 in the cell inner membrane. From the subcellular localization illustrated in Fig. 4c, the high concentration of DEPs in the cytoplasm signifies their involvement in essential metabolic and biosynthetic processes within the cell. Proteins within the cytoplasm are crucial for various cellular functions, such as enzymatic reactions, protein synthesis, and energy metabolism. The differential expression of proteins in the cytoplasm indicates the dynamic adaptation of MR-1 to environmental changes. The significant presence of DEPs in the membrane and the cell's inner membrane highlights the importance of these proteins in maintaining cellular functions. Membrane proteins participate in crucial cellular functions such as transport of molecules, signal transduction, and biofilm formation. The alteration in membrane protein expression under different conditions, particularly in the bioelectrochemical environment, reflects the intricate regulatory mechanisms to support the cell's response to the degradation processes [40]. Furthermore, the

identification of DEPs in multipass membranes underscores their vital role in facilitating electron transfer and transfer of information and molecules across biological membranes [41]. These proteins are integral to electron transport chains and redox reactions, playing a fundamental role in the generation of bioelectricity and the adaptation of *S. oneidensis* MR-1 to the BES.

Functional enrichment analysis was conducted on the DEPs using GO to identify the BPs, CCs and MFs that are enriched in the dataset (Fig. 5a-c). Functional enrichment analysis using GO terms showed that the DEPs were predominantly involved in various metabolic, biosynthetic, catabolic, cellular, and transport processes. GO level 2 of the BP, CC and MF are shown in Fig. S5. An analysis of the protein-protein interaction (PPI) network provided a framework for deciphering the functional relationships between DEPs and their potential interactions (Fig. S6). The analysis revealed that DEPs formed highly interconnected clusters within specific protein groups, which could have a significant impact on the degradation of SMX. The PPI network also reveals the significant correlation between proteins involved in glycolysis such as Enolase and fba with other nodes involved in the metabolism pathway. This indicates that SMX may be broken down to yield a carbon-containing intermediate and function as a potential source of carbon for energy production through glycolysis. Besides, these proteins were also found to be upregulated. The upregulation of these proteins involved in glycolysis provides insights into how *S. oneidensis* MR-1 is adapting its metabolic

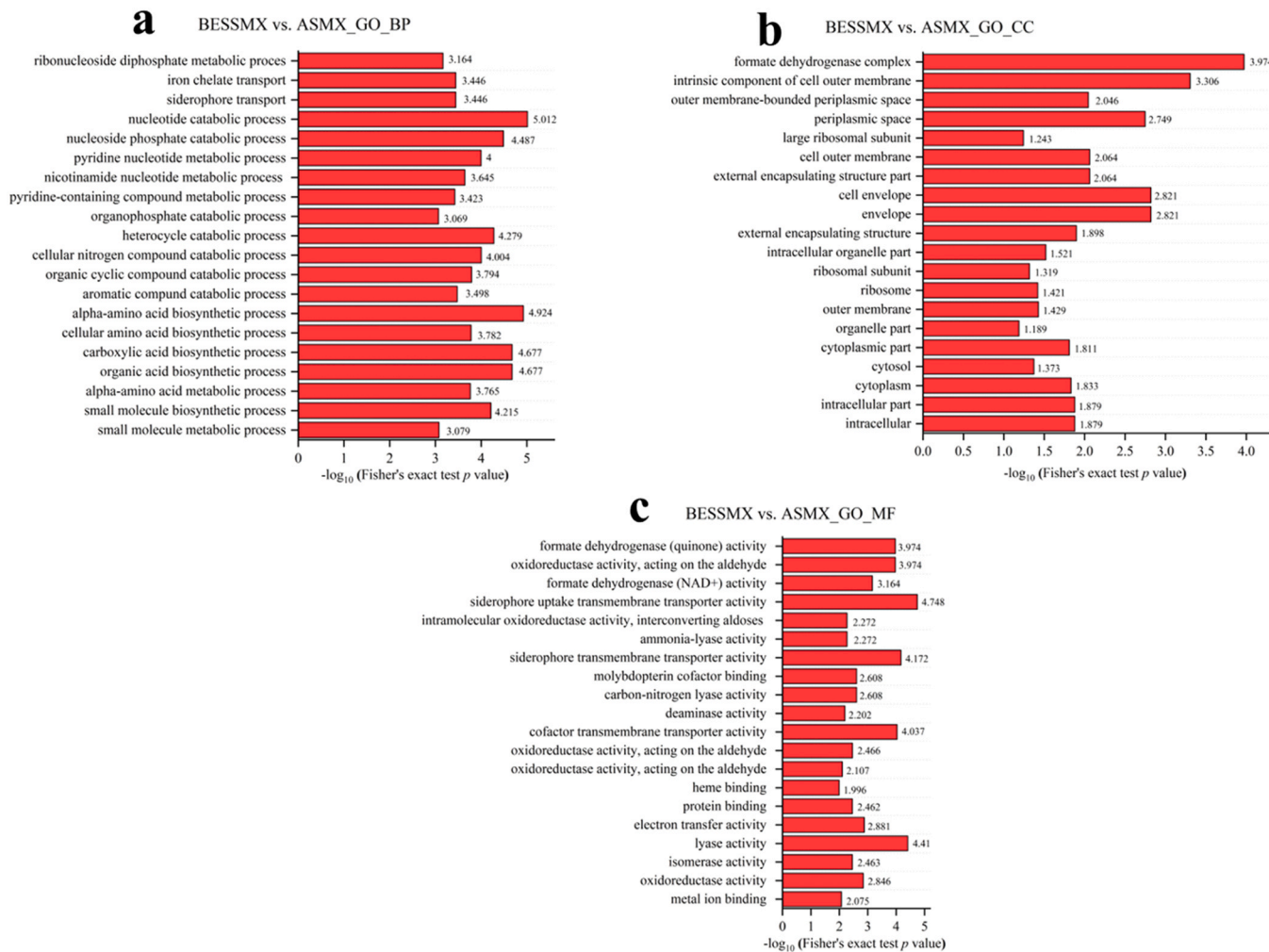


**Fig. 5.** Protein annotation results of top 20 GO counts. (a) Biological process (BP); (b) Cellular component (CC); (c) Molecular functions (MF).

strategies to efficiently degrade contaminants like SMX while meeting its energy demands. The densely connected modules of upregulated proteins were found to be associated with various metabolic processes, including histidine metabolism, purine metabolism, pyrimidine metabolism, nitrogen metabolism, glycine-serine-threonine metabolism, and others.

For this study, the key proteins involved in SMX degradation and EET are of particular attention. The proteins were identified based on the analysis of the expressed proteins. The DEPs related to energy metabolism including ribosomal protein and ABC transporter ATP-binding protein were significantly overexpressed, enhancing the survival and degradation capability of *S.oneidensis* MR-1. Previous studies have shown that the sad genes namely sadA, sadB and sadC gene clusters are responsible for the breakdown of sulfonamides [42]. However, according to the proteomic analysis results of this study, sadA, sadB, and sadC were absent among the DEPs. Nevertheless, there was the upregulation of SMX degrading proteins such as S-ribosyl homocysteine lyase (luxS), Deoxyribose-phosphate aldolase (deoC), and Amidohydrolase. These proteins have been confirmed in the study by Liu et al. [42] to mainly participate in C-S cleavage, S-N hydrolysis and isoxazole ring cleavage. *S. oneidensis* MR-1 seem to employ lactate as a precursor to produce NADH through the tricarboxylic acid (TCA) cycle. The generated NADH is then channelled through a sequence of enzymatic reactions involving NADH-quinone oxidoreductase (complex I), the quinone pool, cytochrome bc1 complex (complex III), and cytochrome c, ultimately conveying electrons to electron acceptors. Additionally, NADH serves as a coenzyme and electron carrier, playing a crucial role in cellular

respiration by facilitating the transfer of electrons in redox reactions [43]. In this study, the modulation of crucial proteins that participate in the electron transport system of cytochrome c was significantly upregulated. This suggests that the enhanced degradation of SMX by the bacteria is attributed to the overexpression of key proteins involved in cytochrome c electron transport [43].

The TCA cycle, illustrated in Fig. 6, demonstrates the upregulation of key proteins such as malate dehydrogenase (MDH) and glyceraldehyde-3-phosphate dehydrogenase (G3PDH) related to NADH generation. Big and densely connected modules of nodes of proteins (Fig. S6) linked with oxidative phosphorylation and energy production such as fumarate reductase flavoprotein were seen to have a strong correlation with the proteins involved in ATP such as Succinate-CoA ligase. Likewise, a significant overlap was found between the proteins involved in NADH generation and those involved in ATP. Proteins such as MDH are involved in the citric acid cycle, generating NADH that is then fed into the electron transport chain for ATP production. Therefore, *S. oneidensis* MR-1 can be inferred to have enhanced the production of NADH and ATP, while also promoting EET. Iron is a crucial element that plays a pivotal role in the functional cores of enzymes responsible for electron-producing and transferring reactions, including cytochrome, dehydrogenases, and reductases [44], as such, the capacity of microorganisms to acquire and assimilate iron is essential for their ability to facilitate EET processes. The proteomic analysis data revealed that *S. oneidensis* induced the expression of genes involved in microbial iron uptake, a process that primarily involves the binding of siderophores produced by the microbe to external iron sources, followed by the

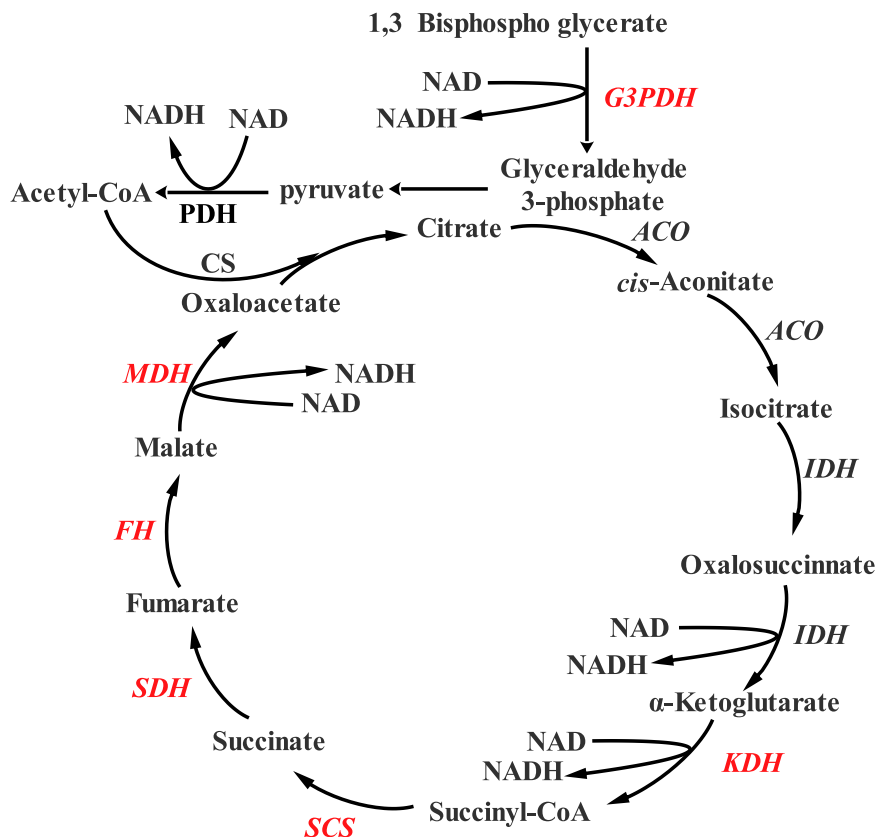


**Fig. 6.** The glycolysis and tricarboxylic acid cycle (TCA) pathway. The protein expressions that are up-regulated are shown in red font. G3PDH: glyceraldehyde-3-phosphate dehydrogenase; PDH: pyruvate dehydrogenase; CS: Citrate synthase; ACO: aconitase; IDH: isocitrate dehydrogenase; KDH: ketoglutarate dehydrogenase; SCS: Succinyl-CoA synthetase; SDH: Succinate dehydrogenase; FH: Fumarate hydratase; MDH: malate dehydrogenase.

transfer of iron-siderophore complexes to the FhuD receptor protein in the inner membrane. This process is facilitated by the porin protein, the TonB-ExbB-ExbD complex, and ultimately leads to the delivery of iron to the cytoplasm, where it can participate in cellular metabolic processes [45]. Consequently, the mechanism underlying *S. oneidensis* MR-1's capacity to facilitate electron transfer during SMX degradation is likely attributed to its superior ability to sequester and translocate periplasmic iron into the cytoplasm, thereby enabling the synthesis of essential enzymes.

#### 3.4. SMX transformation products and proposed degradation pathway

The breakdown products of sulfonamides vary depending on the degradation conditions. Research has focused on the transformation products of SMX, and several studies [46–48] have identified the resulting metabolites. One notable degradation product is 3-Amino-5-methylisoxazole (3A5MI), its accumulation in diverse microorganisms, including *Achromobacter denitrificans* PR1 has been reported in previous studies [49]. This degradation product was also observed during SMX degradation in this study as confirmed by the reference standard. The proposed formula and chemical structures of the eleven transformation products obtained are presented in Table S4. Due to the scarcity of commercially available standards, the structures of two transformation products were verified using reference standards (Fig. S7), while the other nine structures were proposed based on their target mass-to-charge ratios (*m/z*) and by drawing on previous research findings [14,50–53]. Correspondingly four degradation pathways (Pathways I, II, III and IV) were proposed for the degradation of the antibiotic by the bacteria (Fig. 7).

The pathway illustrated in Fig. 7 demonstrates that SMX was initially degraded through the hydroxylation process and this process is

dependent not only on NADH but also fundamentally relies on electron transfer mechanisms facilitated by NADH as electrons are donated during the process [36]. The hydrolysis of the sulfonamide bond has been confirmed to result in N-S (Pathway I) and C-S (Pathway II) bond cleavage [48] indicating that SMX biodegradation through hydroxylation is intrinsically linked to both the availability of NADH and the electron transfer. The cleavage of the N-S bonds (Pathway I) led to two degradation products: TP 99 and TP 173. TP 173 was formed by amidohydrolase. The gene SO\_A0099 encodes an amidohydrolase enzyme with high hydrolase activity, capable of breaking down various chemical bonds, including C-N bonds. The proteomic analysis also confirmed it as part of the upregulated proteins involved in SMX degradation in this study. Afterwards, substitution occurred on TP 99 and this resulted in the amino group being replaced with hydrogen, thus causing TP 99 to be used by microorganisms and further transformation occurred into TP 83. The cleavage of the isoxazole ring of TP 83 led to the formation of TP 90. Since TP 90 has a short chain structure, microbes could find it easy to degrade and this degradation led to the formation of TP 60. TP 60 could further be mineralized by the microbes. Although TP 83 and TP 90 were not detected in this study, this could be due to the rapid conversion of TP 99 to other intermediates such as TP 60.

Though TP 109 and TP 163 (Pathway II) have been confirmed as products formed owing to the C-S bond cleavage [54] TP 109 was not among the detected *m/z* in this study but TP 163 was detected. This could be because the biodegradation pathway of SMX by *S. oneidensis* MR-1 may preferentially cleave the N-S bond (Pathway I), leading to the formation of the detected TP173 and TP 99, while the C-S bond cleavage (Pathway II) may be a less dominant or slower process, resulting in the selective detection of the TP163 [55]. The N-S bond cleavage pathway has been confirmed by previous studies during SMX degradation [56]. In pathway III, TP 147 was generated as a result of the cleavage of the S-C

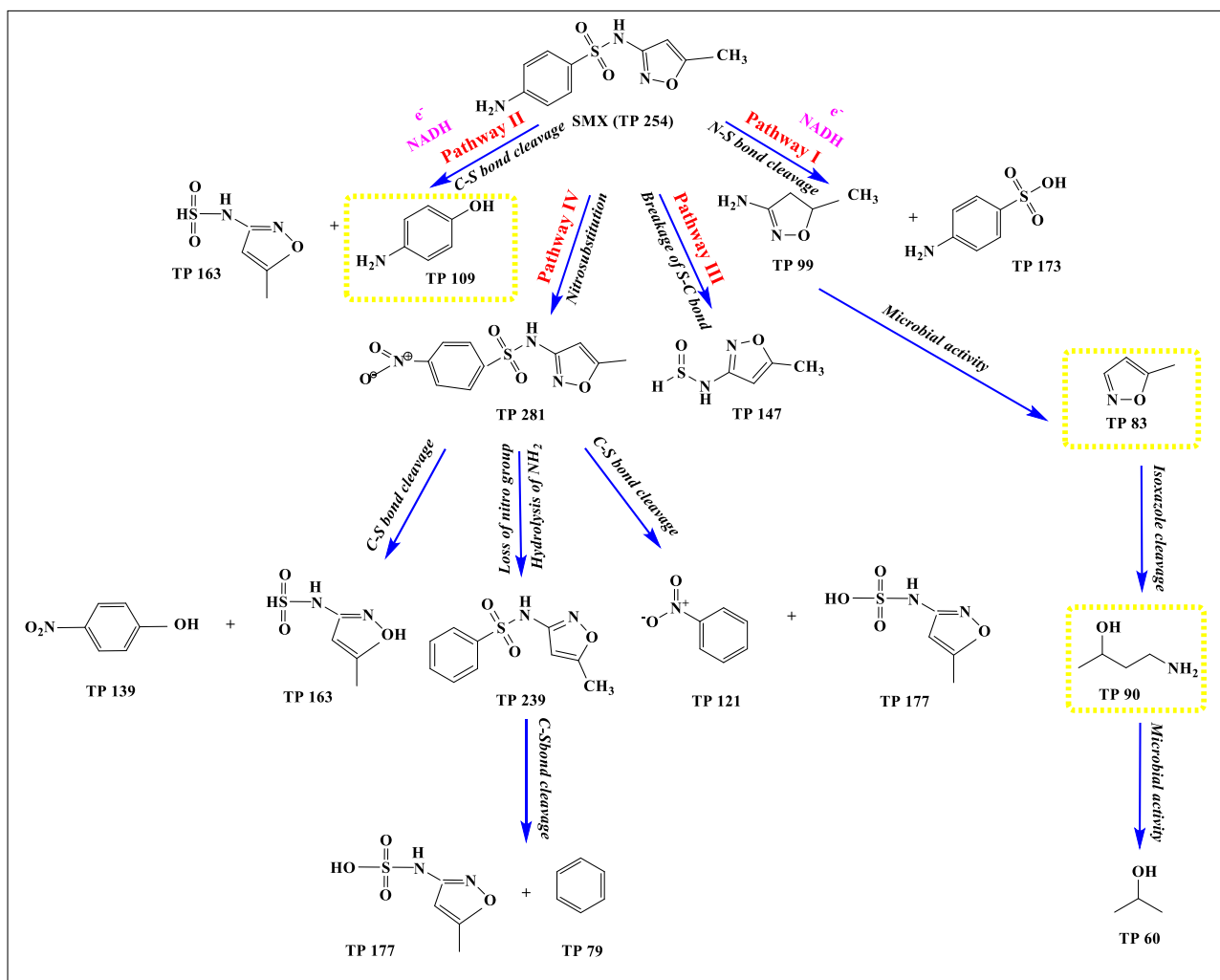


**Fig. 7.** Proposed pathway for sulfamethoxazole removal by *Shewanella oneidensis* MR-1. The yellow rectangle highlights the possible transformation products of SMX not identified by LC-MS/MS.

bond catalyzed by S-ribosyl homocysteine lyase encoded by gene luxS. The luxS gene was also among the upregulated proteins involved in SMX degradation as confirmed by its upregulation in the proteomic analysis in this study. In Pathway IV nitro-substitution was seen as the process taking place on the amino group of aniline and this resulted in the formation of TP 281. Afterwards, TP 281, underwent C-S bond cleavage which led to the degradation products of TP 163, TP 139, TP 177 and TP 121. Subsequently, there was a loss of a nitro group from TP 281 and hydrolysis of the aromatic NH<sub>2</sub>, which led to the production of TP 239 (confirmed with reference standard). Following this was the cleavage of the C-S bond, which led to the formation of TP 177 and TP 79. TP 79 could also be further mineralized by microbes. This degradation experiment produced smaller TPs such as TP 79 and TP 60. This is an indication that SMX was degraded into smaller molecular compounds before it was completely mineralized. These findings may contribute to the design of an efficient method for removing SMX.

### 3.5. Ecotoxicity assessment

The acute and chronic toxicity categories, according to Sun, et al. [57], are presented in Table S5. The toxicity data was divided into four levels: not harmful (LC<sub>50</sub>>100 or EC<sub>50</sub>>100 mg/L; ChV>10 mg/L), harmful (10<LC<sub>50</sub><100 or 10<EC<sub>50</sub><100 mg/L; 1<ChV<10 mg/L), toxic (1<LC<sub>50</sub><10 or 1<EC<sub>50</sub><10 mg/L; 0.1<ChV<1 mg/L) and very toxic (LC<sub>50</sub><1 or EC<sub>50</sub><1 mg/L; ChV<0.1 mg/L). LC<sub>50</sub> which denotes

lethal concentration represents the concentration of a substance (in this case, SMX or its TPs) that is estimated to kill 50 % of the test organisms (Fish, Daphnid and Green algae), during a specified exposure period. EC<sub>50</sub> denotes effective concentration and this represents the concentration of SMX or its TPs that produces a specified effect in 50 % of the test organisms under defined conditions. Unlike LC<sub>50</sub>, which measures lethality, EC<sub>50</sub> is used for determining the effectiveness of substances in eliciting biological responses such as behavioural changes or growth inhibition. ChV denotes chronic toxicity and this is a toxicological measure that indicates the concentration of a substance in an environment below which harmful effects are not expected to occur over a prolonged period. It serves as an important benchmark in environmental risk assessments, helping to establish safety thresholds for aquatic life and other organisms exposed to potentially harmful substances over time. These measures; LC<sub>50</sub>, EC<sub>50</sub>, and ChV are critical in understanding the potential risks posed by chemicals, facilitating comparisons across substances in terms of their toxicity. They are used to inform regulatory decisions, develop safety protocols, and establish exposure limits to protect human health and the environment.

Table S6 illustrates the predicted harmful effect of SMX and its TPs, generated with the ECOSAR program. Fig. 8. illustrates a graphical representation of the acute and chronic effects of SMX and its TPs. As presented in Table S6, the short-term toxicity values of SMX to Fish, Daphnid and Green Algae are given as 266.77, 6.43 and 21.81 mg L<sup>-1</sup>, respectively, while the chronic toxicity values of SMX are given as 5.00,

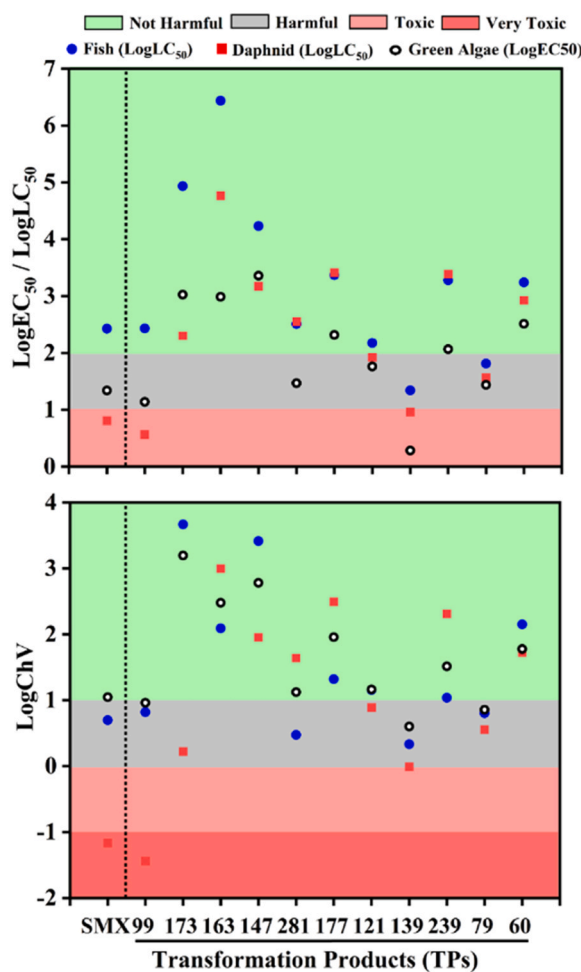


**Fig. 8.** Graphical representation of the acute and chronic impact of SMX and its TPs.

0.06 and  $11.14 \text{ mg L}^{-1}$  for Fish, Daphnid and Algae, respectively. The acute toxicity values of two of the initial transformation products of SMX (TP 99 and TP 173) in pathway I, are given as 270.04, 3.63 and  $13.77 \text{ mg L}^{-1}$  for TP 99 and 86326.91, 200.33 and  $1059.04 \text{ mg L}^{-1}$  for TP 173 for Fish, Daphnid and Green Algae respectively. The chronic toxicity values of TP 99 for Fish, Daphnid and Green Algae are given as 6.58, 0.03 and  $9.16 \text{ mg L}^{-1}$ . While that of TP 173 are given as 4650.41, 1.66 and  $1565.55 \text{ mg L}^{-1}$  respectively. TP 60 which is a lesser TP in that pathway shows an acute toxicity of 1743.47, 844.30 and  $325.70 \text{ mg L}^{-1}$  and a chronic toxicity of 141.25, 52.87 and  $59.84 \text{ mg L}^{-1}$  for Fish, Daphnid and Green Algae respectively. The TP values for the other three pathways are presented in Table S6.

From the results in Fig. 8, it can be inferred that SMX does not have any detrimental effect on Fish but it is toxic to Daphnids and harmful to Green algae as represented under acute toxicity however under chronic toxicity SMX is seen to be harmful to Fish, very toxic to Daphnid and not harmful to Green algae. It is therefore demonstrated that SMX is a toxic pollutant and as such, more attention must be paid to it and its transformation products for aquatic organisms. Under acute toxicity, TP 99 does not have any detrimental effect on Fish but it is toxic to Daphnid and harmful to Green Algae while TP 173 is not harmful to the three organisms. Under chronic toxicity, TP 99 is harmful to Fish, very toxic to Daphnids and harmful to Green Algae but TP 173 has no detrimental effect on Fish and Green Algae but it is harmful to Daphnid. As SMX further degrades to a lesser TP such as TP 60, the toxicity is seen to reduce. These results indicate that this TP 60 is not harmful to the three aquatic organisms under both acute and chronic toxicity. A similar

pattern of reduced toxicity as further degradation occurred, was also observed in the other three degradation pathways. Therefore, it can be said that the initial degradation products though were found to be generally toxic to aquatic organisms but further degradation led to a decline in the toxicity levels of the TPs for the three aquatic organisms. Despite that, the risk of degradation of SMX should still be a major concern.

#### 4. Conclusion

This research elucidates the mechanism of EET in enhancing the degradation of SMX. The result of this study indicates that the degradation rates of SMX in BES are generally higher than in the system without BES across all concentrations tested. *S. oneidensis* MR-1 could degrade concentrations of  $1 \text{ mg L}^{-1}$  of SMX more efficiently (97 %) in the BES compared to the system without BES (69 %). In both cases, the degradation efficiency was found to decrease as the concentration of SMX increased. The possible correlation mechanism between the evolution of extracellular electron transport function and the degradation of SMX by *S. oneidensis* MR-1 was elucidated using the proteomics technique. The proteomics analysis revealed a total of 916 DEPs of which 552 were upregulated and 364 were downregulated. Further analysis revealed that the capacity of *S. oneidensis* MR-1 to degrade SMX is related to the upregulation of protein expressions such as S-ribosyl homocysteine lyase (luxS), Deoxyribose-phosphate aldolase (deoC), and Amidohydrolase. Furthermore, the enhancement of *S. oneidensis* MR-1's EET ability on the electrode was related to the bacteria's ability to enhance NADH and ATP production. Notably, *S. oneidensis* MR-1 was found to stimulate the production of NADH and ATP and facilitate electron transfer to enhance SMX degradation.

#### Funding

This research was funded by grants from the Natural Science Foundation of Fujian for Distinguished Young Scholars (2021J06036), the National Natural Science Foundation of China (22276183), the Youth Innovation Foundation of Xiamen (3502Z20206089), and the Youth Innovation Promotion Association, Chinese Academy of Sciences (Y2022082).

#### CRediT authorship contribution statement

**Yong Xiao:** Writing – review & editing, Supervision, Project administration, Funding acquisition, Conceptualization. **Asmamaw Abat Getu:** Writing – review & editing. **Juvens Sugira Murekezi:** Writing – review & editing. **Geng Chen:** Writing – review & editing, Resources. **Claude Kiki:** Writing – review & editing, Software, Resources. **Collins Chimezie Elendu:** Writing – review & editing, Software, Investigation. **Oluwadamilola Oluwatoyin Hazzan:** Writing – original draft, Validation, Software, Methodology, Investigation, Formal analysis, Data curation, Conceptualization.

#### Declaration of Competing Interest

The authors declare that they have no known competing financial interests or personal relationships that could have appeared to influence the work reported in this paper.

#### Data availability

Data will be made available on request.

#### Appendix A. Supporting information

Supplementary data associated with this article can be found in the online version at doi:10.1016/j.bej.2024.109484.

## References

- [1] C. Mutuku, Z. Gazdag, S. Meleg, Occurrence of antibiotics and bacterial resistance genes in wastewater: resistance mechanisms and antimicrobial resistance control approaches, *World J. Microbiol. Biotechnol.* 38 (9) (2022) 152, <https://doi.org/10.1007/s11274-022-0334-0>.
- [2] T. Katipoglu-Yazan, E. Ubay-Cokgor, D. Orhon, Acute inhibitory impact of sulfamethoxazole on mixed microbial culture: kinetic analysis of substrate utilization biopolymer storage nitrification and endogenous respiration, *Biochem. Eng. J.* 167 (2021) 107911, <https://doi.org/10.1016/j.bej.2020.107911>.
- [3] W. Miran, J. Jang, M. Nawaz, A. Shahzad, D.S. Lee, Biodegradation of the sulfonamide antibiotic sulfamethoxazole by sulfamethoxazole acclimated cultures in microbial fuel cells, *Sci. Total Environ.* 627 (2018) 1058–1065.
- [4] K. McCorquodale-Bauer, R. Grosshans, F. Zvomuya, N. Ciciek, Critical review of phytoremediation for the removal of antibiotics and antibiotic resistance genes in wastewater, *Sci. Total Environ.* (2023) 161876.
- [5] A.B. ENGIN, E.D. ENGIN, A. ENGIN, Effects of co-selection of antibiotic-resistance and metal-resistance genes on antibiotic-resistance potency of environmental bacteria and related ecological risk factors, *Environ. Toxicol. Pharmacol.* (2023) 104081.
- [6] X. Zhang, J. Wang, B. Duan, S. Jiang, Degradation of sulfamethoxazole in water by a combined system of ultrasound/PW12/KI/H2O2, *Sep. Purif. Technol.* 270 (2021) 118790, <https://doi.org/10.1016/j.seppur.2021.118790>.
- [7] Y. Bai, B. Ji, Advances in responses of microalgal-bacterial symbiosis to emerging pollutants in wastewater, *World J. Microbiol. Biotechnol.* 40 (1) (2023) 40, <https://doi.org/10.1007/s11274-023-03819-6>.
- [8] I.A. Vasilidiou, R. Molina, F. Martínez, J.A. Melero, Biological removal of pharmaceutical and personal care products by a mixed microbial culture: sorption, desorption and biodegradation, *Biochem. Eng. J.* 81 (2013) 108–119, <https://doi.org/10.1016/j.bej.2013.10.010>.
- [9] W. Yan, Y. Xiao, W. Yan, R. Ding, S. Wang, F. Zhao, The effect of bioelectrochemical systems on antibiotics removal and antibiotic resistance genes: a review, *Chem. Eng. J.* 358 (2019) 1421–1437.
- [10] K. Yang, I.M. Abu-Reesh, Z. He, Enhancing the degradation of selected recalcitrant organic contaminants through integrated cathode and anode processes in microbial electrochemical systems: a frontier review, *J. Hazard. Mater. Lett.* 3 (2022) 100057.
- [11] D.-C. Hao, X.-J. Li, P.-G. Xiao, L.-F. Wang, The utility of electrochemical systems in microbial degradation of polycyclic aromatic hydrocarbons: discourse, diversity and design, *Front. Microbiol.* 11 (2020) 557400.
- [12] D. Min, L. Cheng, F. Zhang, X.-N. Huang, D.-B. Li, D.-F. Liu, T.-C. Lau, Y. Mu, H.-Q. Yu, Enhancing extracellular electron transfer of *Shewanella oneidensis* MR-1 through coupling improved flavin synthesis and metal-reducing conduit for pollutant degradation, *Environ. Sci. Technol.* 51 (9) (2017) 5082–5089.
- [13] F. Mao, X. Liu, K. Wu, C. Zhou, Y. Si, Biodegradation of sulfonamides by *Shewanella oneidensis* MR-1 and *Shewanella* sp. strain MR-4, *Biodegradation* 29 (2018) 129–140.
- [14] L. Wang, Y. Liu, J. Ma, F. Zhao, Rapid degradation of sulphamethoxazole and the further transformation of 3-amino-5-methylisoxazole in a microbial fuel cell, *Water Res.* 88 (2016) 322–328.
- [15] W. Xue, F. Li, Q. Zhou, Degradation mechanisms of sulfamethoxazole and its induction of bacterial community changes and antibiotic resistance genes in a microbial fuel cell, *Bioresour. Technol.* 289 (2019) 121632, <https://doi.org/10.1016/j.biortech.2019.121632>.
- [16] X. Liu, S. Lu, Y. Liu, Y. Wang, X. Guo, Y. Chen, J. Zhang, F. Wu, Performance and mechanism of sulfamethoxazole removal in different bioelectrochemical technology-integrated constructed wetlands, *Water Res.* 207 (2021) 117814, <https://doi.org/10.1016/j.watres.2021.117814>.
- [17] J. Wang, S. Wang, Microbial degradation of sulfamethoxazole in the environment, *Appl. Microbiol. Biotechnol.* 102 (2018) 3573–3582.
- [18] W. Sun, Z. Lin, Q. Yu, S. Cheng, H. Gao, Promoting extracellular electron transfer of *Shewanella oneidensis* MR-1 by optimizing the periplasmic cytochrome c network, *Front. Microbiol.* 12 (2021), <https://doi.org/10.3389/fmicb.2021.727709>.
- [19] W.-Q. Lin, Z.-H. Cheng, Q.-Z. Wu, J.-Q. Liu, D.-F. Liu, G.-P. Sheng, Efficient enhancement of extracellular electron transfer in *Shewanella oneidensis* MR-1 via CRISPR-mediated transposase technology, *ACS Synth. Biol.* (2024), <https://doi.org/10.1021/acssynbio.4c00240>.
- [20] R. Han, X. Li, Y. Wu, F. Li, T. Liu, In situ spectral kinetics of quinone reduction by c-type cytochromes in intact *Shewanella oneidensis* MR-1 cells, *Colloids Surf. A: Physicochem. Eng. Asp.* 520 (2017) 505–513, <https://doi.org/10.1016/j.colsurfa.2017.02.023>.
- [21] C. Kiki, A. Rashid, Y. Zhang, X. Li, T.-Y. Chen, A.B.E. Adéoye, P.O. Peter, Q. Sun, Microalgal mediated antibiotic co-metabolism: Kinetics, transformation products and pathways, *Chemosphere* 292 (2022) 133438.
- [22] W. Zhu, J.W. Smith, C.-M. Huang, Mass Spectrometry-Based Label-Free Quantitative Proteomics, *BioMed. Res. Int.* 2010 (1) (2010) 840518, <https://doi.org/10.1155/2010/840518>.
- [23] E. Pranckevičienė, Gene Prioritization Using Semantic Similarity, in: S. Ranganathan, M. Gribskov, K. Nakai, C. Schönbach (Eds.), *Encyclopedia of Bioinformatics and Computational Biology*, Academic Press, Oxford, 2019, pp. 898–906.
- [24] J.A. Blake, M.A. Harris, The gene ontology (GO) project: structured vocabularies for molecular biology and their application to genome and expression analysis, *Curr. Protoc. Bioinforma.* 00 (1) (2003) 7.2.1–7.2.8, <https://doi.org/10.1002/0471250953.bi0702s00>.
- [25] M. Kanehisa, S. Goto, KEGG: Kyoto encyclopedia of genes and genomes, *Nucleic Acids Res.* 28 (1) (2000) 27–30, <https://doi.org/10.1093/nar/28.1.27>.
- [26] R.L. Tatusov, M.Y. Galperin, D.A. Natale, E.V. Koonin, The COG database: a tool for genome-scale analysis of protein functions and evolution, 33–6, *Nucleic Acids Res* 28 (1) (2000), <https://doi.org/10.1093/nar/28.1.33>.
- [27] B. Jebalbarezi, R. Dehghanzadeh, S. Sheikhi, N. Shahmahdi, H. Aslani, A. Maryamabadi, Oxidative degradation of sulfamethoxazole from secondary treated effluent by ferrate(VI): kinetics, by-products, degradation pathway and toxicity assessment, *J. Environ. Health Sci. Eng.* 20 (1) (2022) 205–218, <https://doi.org/10.1007/s40201-021-00769-9>.
- [28] C. Kiki, A. Rashid, Y. Wang, Y. Li, Q. Zeng, C.-P. Yu, Q. Sun, Dissipation of antibiotics by microalgae: kinetics, identification of transformation products and pathways, *J. Hazard. Mater.* 387 (2020) 121985, <https://doi.org/10.1016/j.jhazmat.2019.121985>.
- [29] N. Guo, Y. Wang, L. Yan, X. Wang, M. Wang, H. Xu, S. Wang, Effect of bioelectrochemical system on the fate and proliferation of chloramphenicol resistance genes during the treatment of chloramphenicol wastewater, *Water Res.* 117 (2017) 95–101.
- [30] H. Song, W. Guo, M. Liu, J. Sun, Performance of microbial fuel cells on removal of metronidazole, *Water Sci. Technol.* 68 (12) (2013) 2599–2604.
- [31] B. Xie, H. Liang, H. You, S. Deng, Z. Yan, X. Tang, Microbial community dynamic shifts associated with sulfamethoxazole degradation in microbial fuel cells, *Chemosphere* 274 (2021) 129744.
- [32] D. Fernández-Villa, M.R. Aguilar, L. Rojo, Folic acid antagonists: antimicrobial and immunomodulating mechanisms and applications, *Int. J. Mol. Sci.* 20 (20) (2019), <https://doi.org/10.3390/ijms20204996>.
- [33] Y. Xiao, G. Chen, Z. Chen, R. Bai, B. Zhao, X. Tian, Y. Wu, X. Zhou, F. Zhao, Interspecific competition by non-exoelectrogenic *Citrobacter freundii* An1 boosts bioelectricity generation of exoelectrogenic *Shewanella oneidensis* MR-1, *Biosens. Bioelectron.* 194 (2021) 113614, <https://doi.org/10.1016/j.bios.2021.113614>.
- [34] A. Kouzuma, T. Kasai, A. Hirose, K. Watanabe, Catabolic and regulatory systems in *Shewanella oneidensis* MR-1 involved in electricity generation in microbial fuel cells, *Front. Microbiol.* 6 (2015), <https://doi.org/10.3389/fmicb.2015.00609>.
- [35] K.C. Ford, M.A. TerAvest, The electron transport chain of *Shewanella oneidensis* MR-1 can operate bidirectionally to enable microbial electrosynthesis, *Appl. Environ. Microbiol.* 90 (1) (2024) e01387-23, <https://doi.org/10.1128/aem.01387-23>.
- [36] B. Ricken, B.A. Kolvenbach, C. Berges, D. Benndorf, K. Kroll, H. Strnad, R. Vlček, F. Adaiko, P. Hammes, A. Shahgaldian, H.-P.E. Schäffer, P.F.X. Kohler, Corvini, FMNH2-dependent monoxygenases initiate catabolism of sulfonamides in *Microbacterium* sp. strain BR1 subsisting on sulfonamide antibiotics, *Sci. Rep.* 7 (1) (2017) 15783, <https://doi.org/10.1038/s41598-017-16132-8>.
- [37] A. Surazynski, S.P. Donald, S.K. Cooper, M.A. Whiteside, K. Salnikow, Y. Liu, J. M. Phang, Extracellular matrix and HIF-1 signaling: the role of prolidase, *Int. J. Cancer* 122 (6) (2008) 1435–1440.
- [38] M.E. Brosnan, J.T. Brosnan, Histidine metabolism and function, *J. Nutr.* 150 (Suppl 1) (2020) 2570s–2575s, <https://doi.org/10.1093/jn/nxaa009>.
- [39] S.K. Spaans, R.A. Weusthuis, J. Van Der Oost, S.W. Kengen, NADPH-generating systems in bacteria and archaea, *Front. Microbiol.* 6 (2015), <https://doi.org/10.3389/fmicb.2015.00742>.
- [40] X. Cai, L. Huang, G. Yang, Z. Yu, J. Wen, S. Zhou, Transcriptomic, proteomic, and bioelectrochemical characterization of an exoelectrogen *Geobacter* soli grown with different electron acceptors, *Frontiers in Microbiology* 9 (2018) 333696. <https://doi.org/10.3389/fmicb.2018.01075>.
- [41] H. Wu, L. Smalinskaite, R.S. Hegde, EMC rectifies the topology of multipass membrane proteins, *Nat. Struct. Mol. Biol.* 31 (1) (2024) 32–41, <https://doi.org/10.1038/s41594-023-01120-6>.
- [42] X. Liu, J. Chen, Y. Liu, Z. Wan, X. Guo, S. Lu, D. Qiu, Sulfamethoxazole degradation by *Pseudomonas* silesiensis F6a isolated from bioelectrochemical technology-integrated constructed wetlands, *Ecotoxicol. Environ. Saf.* 240 (2022) 113698, <https://doi.org/10.1016/j.ecoenv.2022.113698>.
- [43] C. Zhao, Y. Li, X. Li, H. Huang, G. Zheng, Y. Chen, Biological removal of sulfamethoxazole enhanced by *s. oneidensis* mr-1 via promoting nadh generation and electron transfer and consumption, *J. Hazard. Mater.* 426 (2022) 127839.
- [44] C. Mateo, Iron-Containing Enzyme Catalysts, *Iron Catal.* (2021) 97–125.
- [45] M. Fujita, K. Mori, H. Hara, S. Hishiyama, N. Kamimura, E. Masai, A TonB-dependent receptor constitutes the outer membrane transport system for a lignin-derived aromatic compound, *Commun. Biol.* 2 (1) (2019) 432, <https://doi.org/10.1038/s42003-019-0676-z>.
- [46] X. Wang, J. Li, C. Zhang, M. Xue, H. Xie, Degradation products and transformation pathways of sulfamethoxazole chlorination disinfection by-products in constructed wetlands, *Environ. Res.* 249 (2024) 118343, <https://doi.org/10.1016/j.envrres.2024.118343>.
- [47] F. Bilea, C. Bradu, M. Cicirica, A.V. Medvedovici, M. Magureanu, Plasma treatment of sulfamethoxazole contaminated water: intermediate products, toxicity assessment and potential agricultural reuse, *Sci. Total Environ.* 909 (2024) 168524, <https://doi.org/10.1016/j.scitotenv.2023.168524>.
- [48] Y. Cheng, W. Li, D. Zhang, J. Zhang, F. Zhang, H. Liu, M. Luo, S. Yang, Hydrolysis of sulfamethoxazole in the hyporheic zone: kinetics, factors and pathways, *Environ. Technol.* (2023) 1–14, <https://doi.org/10.1080/09593330.2023.2283402>.
- [49] P.J. Reis, A.C. Reis, B. Ricken, B.A. Kolvenbach, C.M. Manaia, P.F. Corvini, O. C. Nunes, Biodegradation of sulfamethoxazole and other sulfonamides by *Achromobacter denitrificans* PR1, *J. Hazard. Mater.* 280 (2014) 741–749.
- [50] B. Jiang, A. Li, D. Cui, R. Cai, F. Ma, Y. Wang, Biodegradation and metabolic pathway of sulfamethoxazole by *Pseudomonas psychrophila* HA-4, a newly

isolated cold-adapted sulfamethoxazole-degrading bacterium, *Appl. Microbiol. Biotechnol.* 98 (2014) 4671–4681.

[51] B. Ricken, P.F. Corvini, D. Cichocka, M. Parisi, M. Lenz, D. Wyss, P.M. Martínez-Lavanchy, J.A. Müller, P. Shahgaldian, L.G. Tulli, *Ipo-hydroxylation and subsequent fragmentation: a novel microbial strategy to eliminate sulfonamide antibiotics*, *Appl. Environ. Microbiol.* 79 (18) (2013) 5550–5558.

[52] E. Müller, W. Schüssler, H. Horn, H. Lemmer, *Aerobic biodegradation of the sulfonamide antibiotic sulfamethoxazole by activated sludge applied as co-substrate and sole carbon and nitrogen source*, *Chemosphere* 92 (8) (2013) 969–978.

[53] N. Puhlmann, O. Olsson, K. Kümmerer, *Transformation products of sulfonamides in aquatic systems: lessons learned from available environmental fate and behaviour data*, *Sci. Total Environ.* 830 (2022) 154744.

[54] B. Zhang, Y. He, W. Shi, L. Liu, L. Li, C. Liu, P.N.L. Lens, *Biotransformation of sulfamethoxazole (SMX) by aerobic granular sludge: removal performance, degradation mechanism and microbial response*, *Sci. Total Environ.* 858 (2023) 159771, <https://doi.org/10.1016/j.scitotenv.2022.159771>.

[55] A. Wetzel, A.M. Jones, *Electrically driven N(sp<sub>2</sub>)-C(sp<sub>2/3</sub>) bond cleavage of sulfonamides*, *ACS Sustain. Chem. Eng.* 8 (8) (2020) 3487–3493, <https://doi.org/10.1021/acssuschemeng.0c00387>.

[56] S.-Q. Tian, L. Wang, Y.-L. Liu, T. Yang, Z.-S. Huang, X.-S. Wang, H.-Y. He, J. Jiang, J. Ma, *Enhanced permanganate oxidation of sulfamethoxazole and removal of dissolved organics with biochar: formation of highly oxidative manganese intermediate species and in situ activation of biochar*, *Environ. Sci. Technol.* 53 (9) (2019) 5282–5291.

[57] J. Sun, R. Chu, Z.U.H. Khan, *A theoretical study on the degradation mechanism, kinetics, and ecotoxicity of metronidazole (MNZ) in •OH- and SO<sub>4</sub>(•)-assisted advanced oxidation processes*, *Toxics* 11 (9) (2023), <https://doi.org/10.3390/toxics11090796>.